5th International Workshop on Heat/Mass Transfer Advances
for Energy Conservation and Pollution Control
August 13-16, 2019, Novosibirsk, Russia

Simulation of flows with phase transitions and heat transfer using mesoscopic methods

A L Kupershtokh[1] and D A Medvedev[2]

[1] National Research Novosibirsk State University, 2 Pirogova str., Novosibirsk, 630090, Russia
[2] Lavrentyev Institute of Hydrodynamics SB RAS, 15 Lavrentyev prosp., Novosibirsk, 630090, Russia

E-mail: skn@hydro.nsc.ru

Abstract. We use mesoscopic lattice Boltzmann and phase-field methods to simulate the growth of crystals from supercooled melt in the presence of melt convection and the behavior of a pinned droplet under the action of the electric field. In the first problem, the flow influences significantly the shape and the stability of growing patterns, leading to the enhanced development of fingers in the direction opposite to the flow. In the second problem, after the application of the electric field, the droplet begins to elongate in the field direction and the oscillations are produced. These oscillations decay in time due to a viscosity of a fluid. After several oscillations, the droplet acquires its equilibrium shape. The contact angle is essentially reduced compared to the case without an electric field.

1. Introduction

Flows of fluid with phase transitions (liquid-solid and liquid-vapor) are very important for both science and industry. Simulation of such flows is a complicated problem due to the evolution of phase boundaries. Mesoscopic methods that avoid boundary tracking are very promising for these applications.

In the present paper, we consider two problems. The first one is the growth of dendrites in the presence of fluid convection. This is a free boundary problem where boundary conditions need to be imposed at the surface with the shape which changes in time. In this case, the phase-field method is currently the choice for simulating the phase transformation [1]. Being mesoscopic by nature, this method is naturally combined with the lattice Boltzmann (LB) method for fluid flow simulation [2].

The second problem is the non-stationary three-dimensional dynamics of a pinned dielectric droplet in an electric field. Here, there is a complex interplay between the forces acting on the liquid (electric forces, gravity forces, surface tension, wetting of the substrate). These forces affect the shape of the droplet boundary. On the other hand, the distribution of the electric field, the electric and the capillary forces are determined by the droplet shape. Again, the mesoscopic LB method is very promising for simulating this process.

2. Lattice Boltzmann method

Lattice Boltzmann method considers the fluid flows as an ensemble of pseudoparticles that can move along the links of the 3D lattice with possible velocity vectors $\mathbf{c}_k$. We use the D3Q19 LB model ($k = 0,\ldots,18$). The distribution functions N_k in each node are the main variables which are transferred

to the neighbor nodes of 3D lattice in accordance with the characteristics of differential equations $\mathbf{e}_k = \mathbf{c}_k \Delta t$. Then, the distribution functions are changed in a node due to the collision operator with the relaxation time τ. The evolution equation for the distribution functions has the form

$$N_k(\mathbf{x} + \mathbf{c}_k \Delta t, t + \Delta t) = N_k(\mathbf{x}, t) + (N_k^{eq}(\rho, \mathbf{u}) - N_k(\mathbf{x}, t))/\tau + \Delta N_k . \quad (1)$$

The hydrodynamic variables (the density ρ and the velocity $\mathbf{u}$) can be calculated as the moments of the distribution functions $\rho = \sum_{k=0}^{b} N_k$ and $\rho\mathbf{u} = \sum_{k=1}^{b} \mathbf{c}_k N_k$. The process repeats at every time step. The actions of volume forces are taken into account as a change of distribution functions ΔN_k using the Exact Difference Method [3,4]. The pseudopotential method is used to simulate the liquid-vapor phase transition [5,6]. The total force acting on the fluid in a node from the matter in neighbor nodes has the form $\mathbf{F} = -\nabla(P(\rho, T) - \rho\theta)$, where $P(\rho, T)$ is the equation of fluid state.

3. Growth of dendrites

We simulate the thermally controlled growth of dendrites in the presence of fluid convection. The phase-field method [1] is used to calculate the phase transformation. The heat transport (convective and by heat conduction) is simulated using the additional LB component with zero mass (passive scalar) [7,8] taking into account the latent heat released during solidification. The symmetric model is used; the thermal diffusivity and the density of the liquid and the solid phases are the same. The solid-liquid interaction is described by dissipative forces acting in partially filled regions [9,10]. The two-dimensional case is considered with the four-fold anisotropy of the surface tension $\sigma = \sigma_0(1 + \varepsilon \cos 4\theta)$, ε is the degree of anisotropy. The growth of patterns is determined by the surface stiffness, which is defined as $\sigma + d^2\sigma/d\theta^2 = \sigma_0(1 - 15\varepsilon \cos 4\theta)$. The kinetic undercooling is neglected.

Figure 1 shows the simulation results for the growth of patterns in a shear flow (flow is directed from left to right). The left panel presents the results for different flow velocities for the non-dimensional initial undercooling Δ = 0.7 ($\Delta = c_p(T_m - T_0)/L$ where c_p is the specific heat, T_m is the melting temperature, and L is the latent heat of melting), the anisotropy of surface stiffness 15ε = 0.15. The reduced velocity is calculated as $\tilde{U} = Ud_0/D$, where $d_0 = \sigma_0 c_p T_m / L^2$ is the average capillary length with the average surface tension σ_0, D is the thermal diffusivity. The Prandtl number is Pr = ν/D = 1.78. Here, ν is the kinematic viscosity of the melt. Contours represent the boundary of the growing pattern at a different time (the difference between neighbor contours is 50-time steps). For these values of undercooling and anisotropy, the pattern shape is dendritic. With the increase of the flow velocity, the arm perpendicular to the flow direction is somewhat inclined to the inflow direction. Also, the growth of side branches at the upstream side is enhanced due to the supply of cold melt.

When the initial undercooling is increased to 0.8 keeping the same value of anisotropy, a seaweed pattern is obtained which consists of pair fingers (doublons), which is shown in the right panel of Fig. 1. Here, the increment between neighbor contours is 20-time steps. In this case, the influence of flow is much more pronounced. The perpendicular arm bends upstream and becomes parallel to the flow for high flow velocity. The additional side branches also appear.

Simulation of the crystal growth from the melt with natural thermal convection shows the enhanced propagation of arms pointing downwards and the hindering of upward arms. This effect is also due to the supply of cold melt in the first case and heated liquid in the second case.

In the case of a parallel flow, the growth of the finger is enhanced when the flow velocity increases, and the tip radius becomes smaller. For higher flow velocity, however, the sidebranching is observed and the instability of a needle crystal. For high undercooling, the increase of the flow velocity leads to the selection of doublons instead of dendrites.

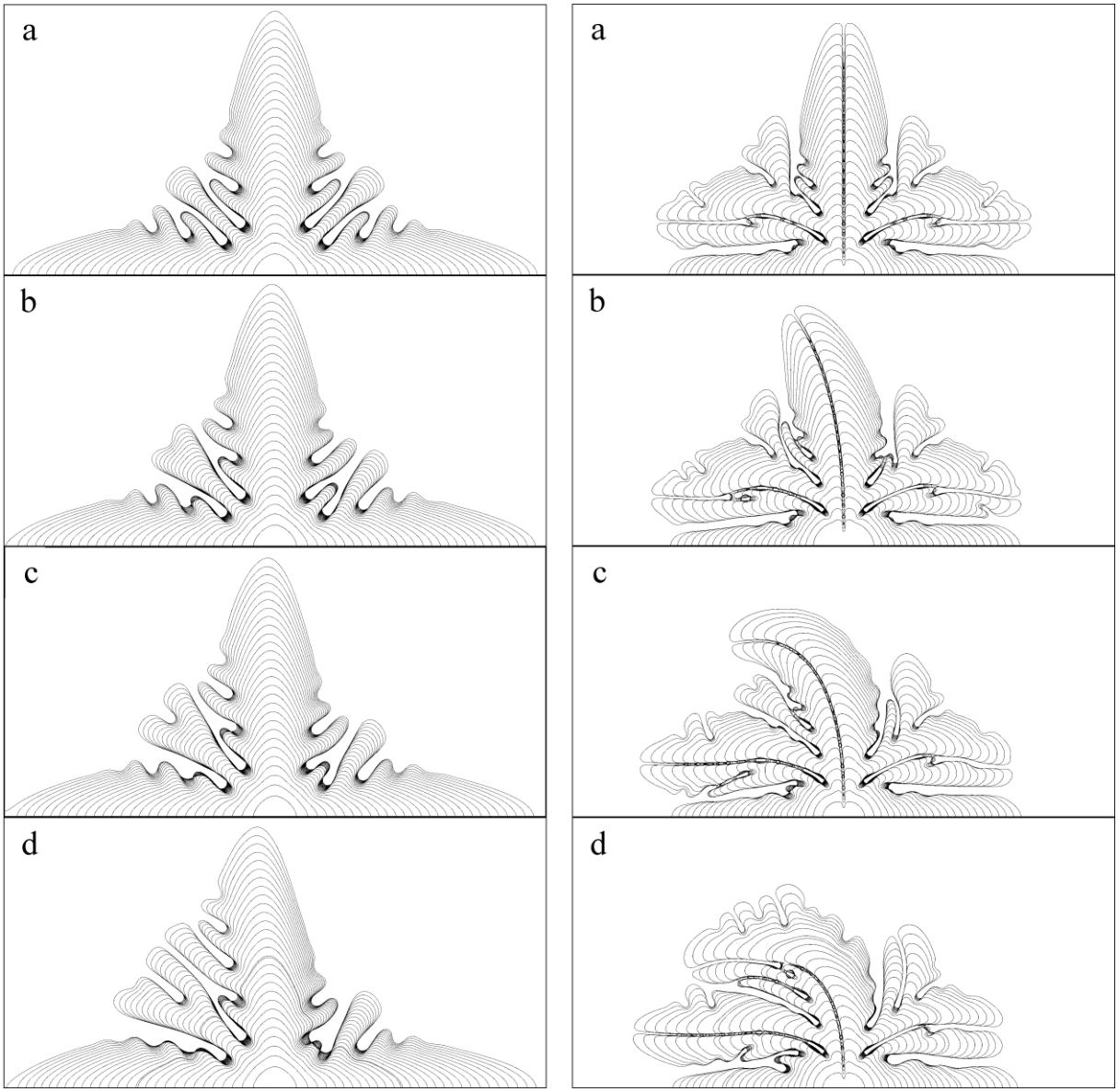

Fig. 1. Left: dendrite in a shear flow. Reduced velocity $\widetilde{U}=0$ (a), 0.0123 (b), 0.0247 (c), 0.0493 (d). Right: seaweed pattern in a shear flow. Reduced velocity $\widetilde{U}=0$ (a), 0.0247 (b), 0.0493 (c), 0.0987(d).

4. Dielectric droplet in an electric field

We also simulate the non-stationary three-dimensional dynamics of dielectric droplets in the electric field. The LB method is used for simulations of the pinned droplet. The position of a contact line for pinned droplet does not move. The van der Waals equation of state in the reduced variables is used for two-phase fluids in accordance with [6]. The dielectric permittivity of a liquid is $\varepsilon_l = 2.3$. The value of the Bond number $\mathrm{Bo} = \rho g R_0^2 / \sigma$ is equal to 0.67. The electrical Bond number $\mathrm{Bo}_e = \varepsilon_0 (\varepsilon_l - 1) E^2 R_0 / \sigma$ is equal to 18.9. One of the simple models assumes the interaction forces between a fluid node $\mathbf{x}$ and the nearest five nodes on the solid surface in the form

$$\mathbf{F}(\mathbf{x}) = B\Phi(\mathbf{x}) \sum_{k=1}^{5} w_k \Phi_{\mathrm{solid}}(\mathbf{x} + \mathbf{e}_k) \cdot \mathbf{e}_k \qquad (2)$$

Here, $\Phi(\mathbf{x}) = \sqrt{\rho\theta - P(\rho,T)}$. For the pinned droplet, the value $\Phi_{\text{solid}}(\mathbf{x}+\mathbf{e}_k)$ on the solid surface is equal to value $\Phi(\rho_l)$ in the circle of the predefined radius R_0. In general case, the parameter B allows one to control the value of the wettability of the solid surfaces.

We solve Poisson's equation for the distribution of the electric field potential φ between the flat electrodes at each time step using the well-known method of simple iterations. The periodic boundary conditions are used along the x and y coordinates. The value of the potential at the upper boundary of the calculation domain is $\varphi(x, y, L_z) = -V$. At the solid substrate, we have $\varphi(x, y, 0) = 0$. The electric field is calculated as $\mathbf{E} = -\nabla\varphi$.

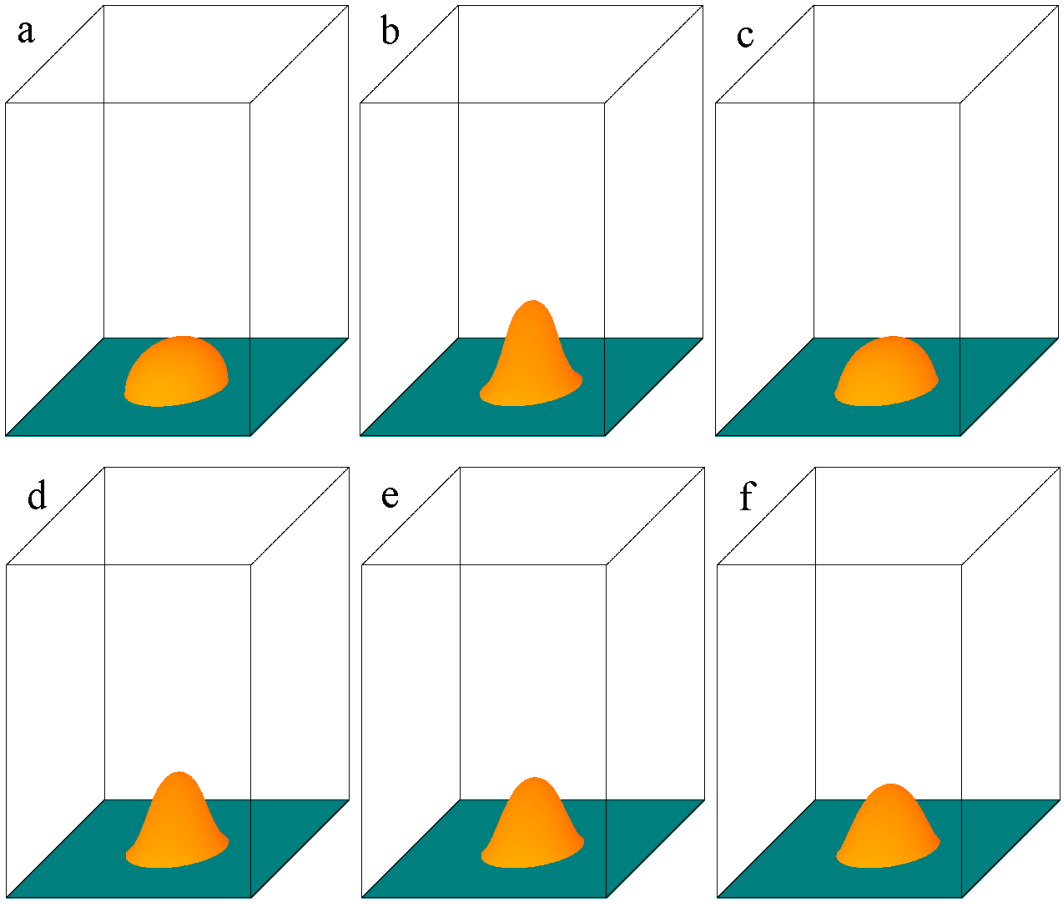

Fig. 2. The dynamics of the pinned droplet on the solid surface in the electric field. The initial hemispherical (a), the first maximum (b), the second maximum (d), the third maximum (e) and the final (f) shapes of the droplet. 3D lattice 400×400×544. $t = 0$ (a), 5400 (b), 11600 (c), 17200 (d), 27400 (e), 114000 (f). $R_0 = 80$, Bo = 0.67, $\varepsilon_l = 2.3$. $\text{Bo}_e = 18.9$, Oh = 0.030.

Initially, the droplet is hemispherical (Fig. 2,a and Fig. 4, curve 1). After the electric field is applied, the droplet begins to elongate in the direction of the electric field. The maximum height of the droplet at the first oscillation is shown in Fig. 2,b. After several oscillations (Fig. 3), the droplet acquires its equilibrium shape. The final shape of the prolate droplet is shown in Fig. 2,f and in Fig. 4 (curve 2). Moreover, for the pinned droplet, the contact angle reduces. The similar experimental results were obtained in [11] for almost hemispherical conducting droplet and for the contact angle without electric field close to 90 degrees. However, the numerical results were obtained in [11] for the pinned droplet only as of the static solution.

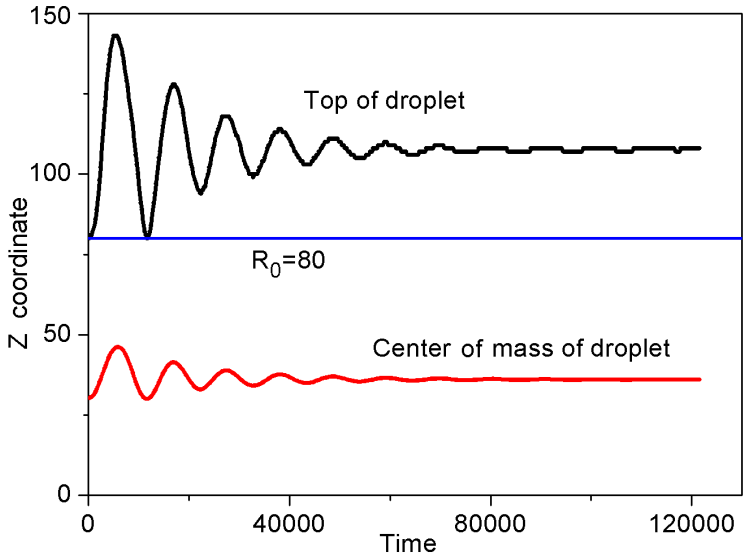

Fig. 3. Time dependences of the positions of the droplet top and the center of mass. $R_0 = 80$, Bo = 0.67, $\varepsilon_l = 2.3$. $\mathrm{Bo}_e = 18.9$, Oh = 0.030.

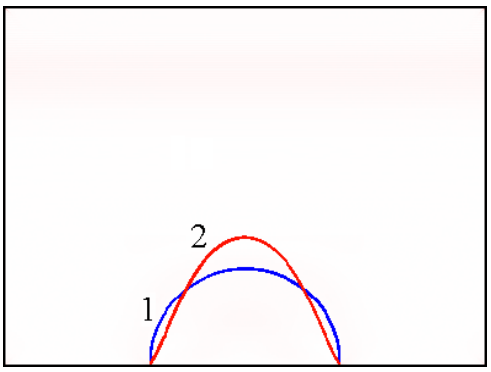

Fig. 4. The part of the central cross-section of the pinned droplet on the solid surface in the electric field. The initial hemispherical (curve 1) and the final (curve 2, $t = 114000$) shapes of the droplet. 3D lattice 400×400×544.

5. Conclusion

We use mesoscopic lattice Boltzmann and phase field methods to simulate flows with phase transitions, liquid-solid, and liquid-vapor ones. First, we investigate the growth of dendrites into a supercooled melt with different flows of liquid. The simulations show the strong influence of the shear flow on the shape and the stability of growing patterns, especially for low anisotropy, when seaweed patterns are present. The growth is enhanced in the direction parallel to the flow and hindered in the opposite direction due to the supply of the cold melt by the flow. For the natural convection and the parallel flow, the flow changes significantly the morphology of the patterns obtained.

Simulations of the behavior of a pinned droplet under the action of electric field reveal the initial oscillations of the droplet due to electric forces. Later, the droplet acquires the elongated shape, and the contact angle is decreased compared with the case without the electric field.

Acknowledgements

The study was supported by the Russian Science Foundation (grant No. 18-19-00538).

References

[1] Karma A and Rappel W-J 1996 Phase-field method for computationally efficient modeling of solidification with arbitrary interface kinetics *Phys. Rev. E* **53** R3017–20
[2] Qian Y H, d'Humières D and Lallemand P 1992 Lattice BGK models for Navier–Stokes equation *Europhys. Lett.* **17**(6) 479–84
[3] Kupershtokh A L 2004 New method of incorporating a body force term into the lattice Boltzmann equation *Proc. 5th Int. EHD Workshop* (University of Poitiers, Poitiers, France) pp 241–6
[4] Kupershtokh A L 2010 Criterion of numerical instability of liquid state in LBE simulations *Computers and Mathematics with Applications* **59**(7) 2236–45
[5] Qian Y H and Chen S 1997 Finite size effect in lattice-BGK models *Int. J. Modern Physics C* **8**(4) 763–71
[6] Kupershtokh A L, Medvedev D A and Karpov D I 2009 On equations of state in a lattice Boltzmann method *Computers and Mathematics with Applications* **58**(5) 965–74
[7] Shan X 1997 Simulation of Rayleigh–Bénard convection using a lattice Boltzmann method *Phys. Rev. E* **55** 2780–8
[8] Kupershtokh A L, Medvedev D A and Gribanov I I 2018 Thermal lattice Boltzmann method for multiphase flows *Phys. Rev. E* **98**(2) 023308
[9] Beckermann C, Diepers H-J, Steinbach I, Karma A and Tong X 1999 Modeling melt convection in phase-field simulations of solidification *J. Comput. Phys.* **154** 468–96
[10] Medvedev D and Kassner K 2005 Lattice Boltzmann scheme for crystal growth in external flows *Phys. Rev. E* **72** 056703
[11] Corson L T, Tsakonas C, Duffy B R, Mottram N J, Sage I C, Brown C V and Wilson S K 2014 Deformation of a nearly hemispherical conducting drop due to an electric field: Theory and experiment *Phys. Fluids* **26**(12) 122106